Check for updates

Received: 23 November 2024 | Revised: 11 April 2025 | Accepted: 20 April 2025

DOI: 10.1111/jne.70041

ORIGINAL ARTICLE

Journal of Neuroendocrinology WILEY

Chronic variable mild stress alters the transcriptome and signaling properties of the anterodorsal bed nucleus of the stria terminalis in a sex-dependent manner

Thomas J. Degroat[1] | Sarah E. Paladino[1] | Benjamin A. Samuels[2] | Troy A. Roepke[1]

[1]Department of Animal Sciences, School of Environmental & Biological Sciences, Rutgers, The State University of New Jersey, New Brunswick, New Jersey, USA

[2]Department of Psychology, Schools of Arts & Sciences, Rutgers, The State University of New Jersey, New Brunswick, New Jersey, USA

Correspondence
Troy A. Roepke, Department of Animal Sciences, School of Environmental & Biological Sciences, Rutgers, The State University of New Jersey, 84 Lipman Drive, Bartlett Hall, New Brunswick, NJ 08901, USA.
Email: ta.roepke@rutgers.edu

Funding information
National Institute of Mental Health, Grant/Award Number: R01MH123544; National Institute of Environmental Health Sciences, Grant/Award Number: P30ES05022

Abstract

Chronic stress is a physiological state marked by dysregulation of the hypothalamic–pituitary–adrenal axis and high circulating levels of stress hormones, such as corticosterone in mice or cortisol in humans. This dysregulated state may result in the development of mood disorders, but the process by which this occurs is still unknown. The bed nucleus of the stria terminalis (BNST) serves as an integration center for stress signaling and is therefore likely an important area for the development of mood disorders. This project utilized a chronic variable mild stress (CVMS) paradigm to persistently stress mice for 6 weeks, followed by RNA-Sequencing of the anterodorsal (ad) BNST and electrophysiology of corticotropin-releasing hormone-expressing cells in the adBNST. Our results show significant sex biases in the transcriptome of the adBNST as well as effects of CVMS on the transcriptome of the adBNST specifically in males. Female-biased genes are related to synaptic transmission, while male-biased genes are related to RNA processing. Stress-sensitive genes in males are related to synaptic transmission and synapse formation. Additionally, electrophysiology data showed that CVMS suppressed the M-current in males but not females. However, CVMS increased the strength of excitatory post-synaptic currents in females but not males. This suggests significant differences in how males and females process chronic stress. It also suggests that the BNST is more sensitive to chronic stress in males than in females.

KEYWORDS
BNST, chronic stress, CRH, M-current, RNA-sequencing

1 | INTRODUCTION

In the central stress response, the major signaling molecules include corticotropin-releasing factor/hormone (CRF/H) and adrenergic neurotransmitters. By contrast, the major stress molecule in the periphery is cortisol in humans and corticosterone in rodent models. When presented with a stressor, the brain must first recognize the stressor through the integration of multiple processing centers, notably the amygdala, paraventricular hypothalamus, and locus coeruleus.[1,2] The amygdala and paraventricular hypothalamus produce CRF/H, while the locus coeruleus produces norepinephrine and responds to CRF/H. CRH from the paraventricular hypothalamus controls the hypothalamic–pituitary–adrenal axis.

Chronic stress refers to a state of dysregulation of these stress-related pathways. During chronic stress, the hypothalamic–pituitary–adrenal axis is overactivated, resulting in constant stress signaling in both the brain and periphery. This can result in permanent changes, such as the development of mood disorders in the brain. While chronic stress and acute stress activate similar signaling pathways, it is known that the two states result in different signaling processes in

 © 2025 British Society for Neuroendocrinology.

the brain. For example, it has been shown that acute stress leads to an increase in CRH receptor expression, possibly related to sensitization, but chronic stress does not cause this.[3] Similarly, chronic and acute stress have differing effects on the expression of CRF in various regions of the brain.[4] This has also been shown to happen to adrenergic pathways as well.[5] Thus, it is important to understand how chronic stress is processed and how that processing is changing the function and neuroanatomy of the brain.

The bed nucleus of the stria terminalis (BNST), a part of the limbic system or extended amygdala, is a region that also produces CRF-mediated output to mood regulation. Many of the previously discussed stress-related regions directly innervate the BNST and, as such, it also can serve as an integration center for the central stress response.[1] This heterogeneous area expresses receptors for various stress-related proteins, including CRF receptors and adrenergic receptors.[6] The BNST is of particular interest for studying chronic stress processing, as previous studies suggest the BNST is only activated through long-context stressors, as demonstrated by an increase in c-fos expression in the BNST only after long-context stressors.[7] Further research has shown that when the BNST is lesioned, only the mice exposed to long-context stressors showed impairment in their behavioral adaptations and conditioning.[8,9]

However, long-context stressors are not the same as chronic stress and therefore, more evidence is necessary to show that the BNST is involved in chronic stress. This has been shown both molecularly and behaviorally. In one study, chronic stress significantly increased the dendritic arborization of the BNST and this appeared to be specific to this region as the central amygdala, another region of the brain important for stress signaling, had no difference in its arborization.[10] Furthermore, another study testing the differing effects of chronic versus acute stress found that only chronic stress resulted in alterations of the long-term potentiation of the BNST that was paired to changes in their behavior.[11] Other studies have shown changes to electrophysiological properties and the transcriptome of specific populations of cells in the BNST after chronic stress.[12]

There are multiple ways to study chronic stress in animal models. Common methods include direct corticosterone injections, social dominance, physical restraint, and pain administration. Each chronic stress paradigm has benefits and drawbacks and should be selected based on the experimental question the researcher is addressing. A chronic variable mild stress (CVMS) paradigm, often also called chronic unpredictable mild stress, was developed in the 1980s and has become a standard of chronic stress research. CVMS uses a randomized schedule of multiple different types of stressors with them frequently being mild in nature though occasionally stronger stressors are used in the schedule.[13] This paradigm is attractive to study chronic stress as it often models naturalistic stressors that a rodent would encounter, such as uncomfortable environments, threats of nearby predators, and social stress. This improves its translatability to humans. Additionally, this paradigm has been validated as a great model for mood disorders as CVMS causes depression-like behaviors in rodents such as learned helplessness or anhedonia which are reversible by treatment with antidepressants.[14–17] Furthermore, this study serves as an expansion and continuation of previously published projects that utilized the CVMS paradigm to better elucidate the effects that this paradigm has in mice.[18,19]

When studying how chronic stress develops into a mood disorder, one must also consider how variability across the sexes influences responses to chronic stress. In clinical research, it has been shown that most mood disorders have a strong gender bias, with major depressive disorder being twice as prevalent in cisgender women than in cisgender men.[20] In animal models, differing responses to chronic stress have also been observed between the sexes. In our previous publication, we found that the response to the CVMS paradigm elicited different responses in avoidance behavior across the sexes and across the estrous cycle.[18] We also previously found that the CVMS paradigm, in a study only using male mice, altered the M-current and excitatory post-synaptic currents (EPSCs) in BNST CRH neurons,[19] but that this paradigm did not alter the M-current in BNST NPY-expressing cells in either sex.[18] Further, when using bulk RNA-Sequencing of the anterodorsal (ad) BNST, we found no effects of CVMS on the transcriptome 18 h after the last stressor.[18] In the current study, we examined the influence of CVMS on CRH excitability, M-current activity, and EPSCs, in both male and female mice, and, due to the transient nature of the transcriptome, on the transcriptome of the adBNST 1 h after the last stressor (wet bedding). We postulate that the earlier collection post-stress would provide better insight into how stressors alter the transcriptome of the adBNST in a sex-specific manner that may lead to the sustained differences in neurophysiology. Our main goal is to characterize how the neurons of the adBNST, especially CRH neurons, respond to chronic stressors across the sexes.

2 | MATERIALS AND METHODS

2.1 | Animals

All procedures were in accordance with National Institutes of Health standards and approved by the Rutgers Institutional Animal Care and Use Committee and agree with ARRIVE's guidelines for reporting animal research. Mice used for all cohorts were adult male and female C57BL/6J mice. Mice used for electrophysiology were bred in house, and mice used for RNA-Sequencing were purchased at 3 weeks of age from Jackson Laboratories (Cat# 000664). For electrophysiology, mice were cross-bred between an Ai14 parent and a corticotropin-releasing hormone (CRH)-Cre parent so that offspring had mutations for both Ai14 and CRH-Cre, resulting in exclusive expression of td-Tomato in CRH-expressing cells. Both Ai14 and CRH-Cre breeding mice were purchased from Jackson Laboratories (Cat # 007914 & 012704, respectively). Control or stress conditions were started at 7–10 weeks of age. Except for stressors, mice were housed in a temperature- and humidity-controlled room (22°C, 30%–70% humidity), on a 12/12 h light/dark cycle, and provided food and water ad libitum. Sample sizes of $n = 7–9$ cells for electrophysiology allowed for detection of effects with a power = 0.8 at $\alpha = 0.05$. This was

13652826, 2025, 8, Downloaded from https://onlinelibrary.wiley.com/doi/10.1111/jne.70041 by Benjamin Samuels - Rutgers University Libraries , Wiley Online Library on [07/11/2026]. See the Terms and Conditions (https://onlinelibrary.wiley.com/terms-and-conditions) on Wiley Online Library for rules of use; OA articles are governed by the applicable Creative Commons License

based on previously published studies in our lab.[18,19,21] RNA-Sequencing was conducted via pooling three biological replicates into a single sample with 15 mice per group, resulting in an ultimate sample of $n = 5$ per group. For electrophysiology mice, they were sacrificed the morning after the last stressor, approximately 18 h later, at 9:00–10:00 am. For the RNA-Sequencing cohorts, mice were euthanized 1 h after the last morning stressor at 10:30–11:30 am. Body weight was collected in the RNA-Sequencing cohort once a week to monitor health and the effects of the CVMS paradigm.

2.2 | Chronic variable mild stress paradigm

The CVMS paradigm is a 6-week schedule of 1–2 minor stressors every day, typically with one morning stressor and one evening stressor. This paradigm follows the same procedure as outlined in our previous publication.[18] Briefly, mice were subjected to the following stressors: 3 or 8 h of humid bedding, 8 h of no bedding, 8 h of replacing bedding with room temperature water, placing the cage on a 45° tilt for 8 h, isolation for 8 h or overnight, exposure to novel mice's dirty cages for 8 h, lights on overnight, 2 or 3 h of dark during the typical light cycle, 5 or 6 bedding changes in a single day, 2-min swim stress in 4°C water, 4-min swim stress in room temperature water, 15-min cold stress, 15 min of predator sounds, and 1 h of restraint stress.

2.3 | RNA-sequencing

To collect tissue for RNA-Sequencing, mice were first anaesthetized via ketamine followed by decapitation. Mice were injected with 0.1 mL of ketamine, and mice were monitored until anesthetization was ensured. All mice were euthanized within 5 min of ketamine injection. Brains were dissected out, sliced, and then microdissected using a dissecting scope and scalpel to isolate the adBNST. The adBNST was collected and pooled bilaterally. Tissue samples from three biological replicates were then pooled prior to RNA extraction and were stored in RNA later at −80°C. RNA was extracted using an RNAqueous Micro Isolation kit (Invitrogen; AM1931). Integrity, concentration, and quality of the RNA samples were analyzed with an Agilent 2100 Bioanalyzer prior to being sent to the JP Sulzberger Columbia Genome Center (New York, NY) for sequencing. All samples sent to JP Sulzberger Columbia Genome Institute were analyzed on an Agilent 2100 Biolanalyzer to ensure that the RNA integrity number (RIN) was greater than 8. No samples were discarded due to low RIN. Libraries were constructed using Illumina TruSeq Stranded mRNA Library Prep Kit with KAPA HiFi HotStart Ready Mix for the final PCR step and were sequenced on an Element AVITI with 100 bp paired-end reads at a depth of 40 million. Resulting fastq files were then analyzed as previously described.[18] RNA-Sequencing had a sample size of $n = 5$ for each group with no outliers. Raw sequencing data can be accessed at GEO GSE281507.

2.4 | Electrophysiology

Electrophysiology was conducted as previously described.[18] Briefly, mice were decapitated without anesthetization between 8:30 am and 10:00 am. The brain was then dissected out and sliced on a VT1000 S vibrating blade microtome (Leica) at 250 nm thickness in a high sucrose artificial cerebral spinal fluid (aCSF) that was prepared in-house (containing in mmol: 208 sucrose, 2 KCl, 26 $NaHCO_3$, 10 glucose, 1.25 NaH_2PO_4, 2 Mg_SO_4 1 $MgCl_2$, 10 HEPES with a pH of 7.35 and osmolarity of 290–310 mOsm). Slices were then allowed to acclimate at room temperature in a bath of continuously oxygenated aCSF (containing in mmol: 124 NaCl, 5 KCl, 2.6 NaH_2PO_4, 2 $MgCl_2$, 2 $CaCl_2$, 26 $NaHCO_3$, 10 glucose with a pH of 7.35 and osmolarity of 290–310). Once acclimated, individual slices were placed in the bath of the electrophysiology rig that contained the same aCSF recipe as the acclimatization chamber but held at 35°C. Individual cells were then selected by fluorescence of the tdTomato (a representative image of the fluorescing CRH+ neurons is available in Figure 3L). A borosilicate pipette backfilled with an internal solution (containing in mmol: 10 NaCl, 128 K-gluconate, 1 $MgCl_2$, 10 HEPES, 1 ATP, 1.1 EGTA, and 0.25 GTP with a 7.35 pH and 290–300 mOsm) was used to patch onto the cell. Membrane values and standard protocol were recorded for every cell and throughout the duration of the patching to ensure the health of the cell. Data collection was done using 1550B Axon Instruments Digidata acquisition system, 700B Axon Instruments Multiclamp amplifier, and pCLAMP software (version 11.1) from Molecular Devices.

Recordings and analysis of the M-current were conducted as previously described.[18] Briefly, slices were first bathed in an aCSF solution that contained 1 μM tetrodotoxin (TTX) (Tocris, Cat. # 1069) and allowed to perfuse for 5 minutes before recording. Under voltage-clamp, a standard deactivation protocol was used to measure K+ currents elicited during 500-ms voltage steps from −30 to −75 mV in 5-mV increments after a 300-ms prepulse to −20 mV. After this baseline recording, XE-991 (Tocris, Cat. # 2000), a selective inhibitor of KCNQ channels, was introduced to the bath at 40 μM and allowed to perfuse for 10 minutes. The same deactivation protocol was then recorded. M-current data was analyzed by Clampfit 11. The M-current is an inhibitory current that acts through voltage-gated K+ channels.[22,23] As it is one of the few currents that are active at physiologically relevant voltages, it has an impact on the likelihood for a cell to fire an action potential.[24] In summation, a strong M-current suggests a cell that is less likely to fire, whereas a weak M-current suggests a cell that is more likely to fire. Representative traces of the M-current can be found in Figure 3A.

EPSC was analyzed on Easy Electrophysiology. EPSCs were detected using the template event detection feature using the deconvolution method with a theta of 4.5. Events were then individually checked to ensure noise was not accidentally counted. Events were then averaged, and the number of events, average amplitude, and average charge (Q), analyzed as the area under the curve for the EPSCs, were recorded. Two 5-minute recordings were done for EPSCs, one in which the slice was in vehicle conditions and one in

13652826, 2025, 8, Downloaded from https://onlinelibrary.wiley.com/doi/10.1111/jne.70041 by Benjamin Samuels - Rutgers University Libraries , Wiley Online Library on [07/11/2026]. See the Terms and Conditions (https://onlinelibrary.wiley.com/terms-and-conditions) on Wiley Online Library for rules of use; OA articles are governed by the applicable Creative Commons License

which Stressin 1 (Tocris, Cat. #1608), a selective agonist of the CRH receptor 1, was introduced to the bath. For this second recording, Stressin 1 was introduced to the bath at a 100 micromolar concentration and allowed to incubate on the slice for 5 minutes before recording. Representative traces of current recording for EPSCs can be found in Figure 4A.

M-current tests had sample sizes of $n = 9$ for control males from six mice, $n = 10$ for stressed males from eight mice, $n = 8$ for control females from six mice, and $n = 9$ for stressed females from eight mice. There were no outliers for M-current. EPSC tests had sample sizes of $n = 7$ for control males from six mice, $n = 8$ for stressed males from seven mice, $n = 8$ for control females from seven mice, and $n = 9$ for stressed females from eight mice. A table of outliers for EPSCs can be found in Table S1. Females were tested only in diestrus to ensure consistent hormone profiles between mice; diestrus was confirmed by vaginal cytology the morning of the electrophysiology recording. Unless otherwise specified, all chemicals were purchased from Sigma-Aldrich.

2.5 | Statistics

Unless otherwise specified, all tests were analyzed using Prism (GraphPad Prism, Version 10, Dotmatics) and used a p-value or adjusted p-value of <0.05 for significance. Body weight tracking and electrophysiology tests were first checked for outliers by the Grubbs' test using a critical value of 0.05 as the cut-off. EPSC data were analyzed by a two-way ANOVA. RNA-Sequencing data was analyzed by DESeq2 on R Studio. Cumulative body weight gain and the IV plots of the M-current recordings were analyzed by a repeated-measures two-way ANOVA. Max peak of the current at −35 mV, resting membrane potential, and change in input resistance were analyzed by a two-way ANOVA. All ANOVAs were followed by Tukey *post-hoc* comparisons.

3 | RESULTS

3.1 | Body weight

Body weight gain was impacted by CVMS exposure in both the males and females; however, the sexes responded differently. In males, body weights between control and stressed counterparts remained consistent for the first 3 weeks, diverging thereafter [main effect of treatment: $F(1, 28) = 10.94$, $p = 0.0026$; interaction effect (Weeks × Treatment): $F(6, 68) = 9.498$, $p < 0.0001$], Figure 1A. After week one, the control males gained 2.6% of their body weight, and stressed males gained 3.3% (not significant [ns]). After week two, control males gained 7.9% while stressed males gained 7.6% (ns). After week three,

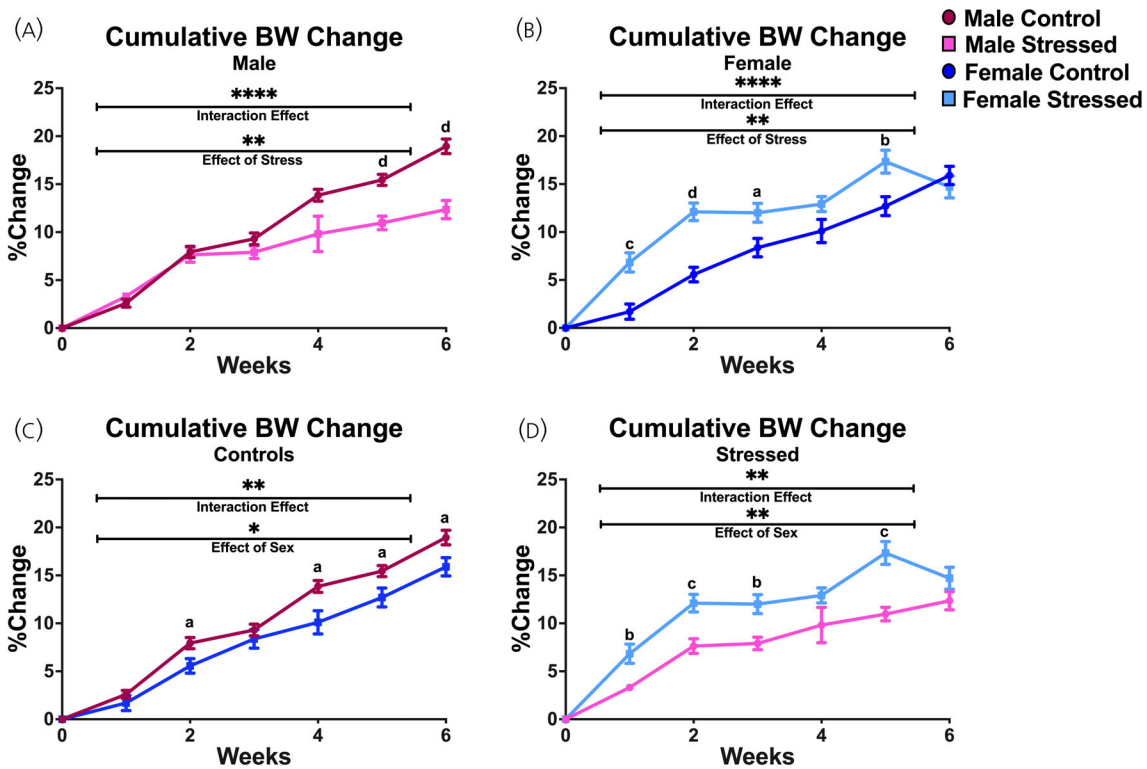


FIGURE 1 Cumulative % change in body weight during the 6-week stress paradigm. (A) Comparison between control males and stressed males. (B) Comparison between control females and stressed males. (C) Comparison between control males and control females. (D) Comparison between stressed males and control females. Analyzed by repeated measures two-way ANOVA. Asterisks with capped lines represent main effects with the comparison written below the capped line. Lower-case letters represent pairwise comparisons. (* = 0.05–0.01, ** = 0.01–0.001, *** = 0.001–0.0001; $a = 0.05$–0.01, $b = 0.01$–0.001, $c = 0.001$–0.0001, $d > 0.0001$).

13652826, 2025, 8, Downloaded from https://onlinelibrary.wiley.com/doi/10.1111/jne.70041 by Benjamin Samuels - Rutgers University Libraries , Wiley Online Library on [07/11/2026]. See the Terms and Conditions (https://onlinelibrary.wiley.com/terms-and-conditions) on Wiley Online Library for rules of use; OA articles are governed by the applicable Creative Commons License

control males gained 9.3% while stressed males gained 7.9% (ns). After week four, control males gained 13.8% while stressed males gained 9.8% (trending, $p = 0.054$). After week five, control males gained 15.5% while stressed males gained 11.0% ($p < 0.0001$). After the final week of stressors, control males gained 19.0% while stressed males gained 12.4% ($p < 0.0001$). This data indicates that CVMS inhibited weight gain, presumably through changes in feeding or metabolism, in male mice.

In females, body weight gain was different at the beginning [main effect of treatment: $F(1, 28) = 8.820$. $p = 0.0061$; interaction effect (Weeks × Treatment): $F(6,168) = 11.42$, $p < 0.0001$], then converged towards the end of the paradigm (Figure 1B). After week one, control females gained 1.7% of their body weight while stressed females gained 6.8% ($p = 0.0004$). After week two, control females gained 5.6% while stressed females gained 12.1% ($p < 0.0001$). After week three, control females gained 8.4% while stressed females gained 12.0% ($p = 0.0135$). After week four, control females gained 10.1% while stressed females gained 12.9% (ns). After week five, control females gained 12.7% while stressed females gained 17.3% ($p = 0.0057$). After the final week of stressors, control females gained 15.9% while stressed females gained 14.7% (ns). For females, data shows that they have a transient increase in body weight gain after exposure to stress, which plateaus under chronic conditions.

When comparing sexes, there are differences in both the control and stress groups. In the control group, males gained weight quicker than females, as expected [sex effect: $F(1, 28) = 5.732$, $p = 0.0236$; interaction effect (Weeks × Sex): $F(6,168) = 3.847$, $p = 0.0013$] (Figure 1C). However, in the stressed groups, the females gained weight quicker than the males [sex effect: $F(1, 28) = 13.17$, $p = 0.0011$; interaction effect (Weeks × Sex): $F(6, 168) = 3.901$, $p = 0.0011$] (Figure 1D). This shows the differing effects of chronic stress on the sexes as the females gained weight quicker because of the stress, whereas the male mice gained weight slower due to stress.

3.2 | adBNST transcriptome

The principal component analysis of all samples used for RNA-Sequencing illustrates that there are no outliers for any groups as all samples fit within their respective 95% confidence interval ovals (Figure 2A). The analysis also finds that males and females are strongly separated, and control male mice are separated from stressed male mice. However, the control and stressed female samples are almost entirely overlapping. There were 248 genes found to be significantly differentially expressed between males and females and a further 216 that were trending ($0.10 > \text{adj. } p > 0.05$) (Figure 2B). Of the significant genes, 116 were male biased while 132 were female biased.

Of the genes varying across sex, male-biased genes of interest included: *Hcrtr1* ($\log_2FC = 1.075$, adj. $p = 0.0240$), the orexin receptor,[25] *Sgk1* ($\log_2FC = 1.045$, adj. $p < 0.0001$), a modulator of neuronal excitability,[26] *Tac2* ($\log_2FC = 0.783$, adj. $p = 0.0167$), the tachykinin/neurokinin B receptor,[27] *Mc4r* ($\log_2FC = 0.712$, adj. $p = 0.0012$), a melanocortin receptor,[28] *Crh* ($\log_2FC = 0.572$, adj. $p = 0.0109$), *Insyn2a* ($\log_2FC = 0.280$, adj. $p = 0.0297$), a modulator of post-synaptic potential,[29] and *Gna13* ($\log_2FC = 0.198$, adj. $p = 0.0254$) which enables dopamine signaling.[30] These differences suggest sex biases in the type and strength of signaling of adBNST neurons as many genes are related to receptors or signaling cascades. A further list of selected male-biased DEGs of interest along with their $\log_2FC$, adjusted *p*-value, and functional relevance can be found in Table 1. A list of all male-biased genes can be found in Table S2.

Female-biased genes of interest included: *Gsg1l* ($\log_2FC = 0.603$, adj. $p = 0.0131$) and *Cacng3* ($\log_2FC = 0.428$, adj. $p = 0.0483$), both regulators of AMPA receptors,[31,32] *Tgfa* ($\log_2FC = 0.530$, adj. $p = 0.0113$), a regulator of neurogenesis,[33] *Camk2n1* ($\log_2FC = 0.443$, adj. $p = 0.0046$), an inhibitor of long-term potentiation,[34] *Cplx1* ($\log_2FC = 0.281$, adj. $p = 0.0423$) and *Cplx2* ($\log_2FC = 0.350$, adj. $p = 0.0297$), both involved in synaptic vesicle exocytosis,[35] *Anks1b* ($\log_2FC = 0.303$, adj. $p = 0.0405$), a modulator of synaptic plasticity,[36] *Comt* ($\log_2FC = 0.215$, adj. $p = 0.0433$), catecholamine metabolism,[37] and *Slc1a2* ($\log_2FC = 0.181$, adj. $p = 0.0397$), a glutamate transporter.[38] This suggests a difference in both the signaling and synaptic plasticity in the adBNST between males and females. A further list of selected female-biased DEGs of interest along with their $\log_2FC$, adjusted *p*-value, and functional relevance can be found in Table 2. A list of all female-biased genes can be found in Table S3.

Comparing control females and stressed females, only 1 gene, *Rbm3*, was found to be differentially regulated, and only 6 further genes were trending (Figure 2D). *Rbm3* was upregulated due to stress ($\log_2FC = 0.436$, adj. $p < 0.0001$). Of the genes altered by stress in males, 217 were differentially regulated, with 57 downregulated by stress and 160 upregulated, and another 301 trending (Figure 2C). Those downregulated by stress included: *Sgk1* ($\log_2FC = -0.842$, adj. $p = 0.0050$),[26] *Slc1a6* ($\log_2FC = -0.552$, adj. $p = 0.0232$), a glutamate transporter,[39] *Crh* ($\log_2FC = -0.485$, adj. $p = 0.0420$), *Vamp1* ($\log_2FC = -0.424$, adj. $p = 0.0196$), involved in synaptic vesicle exocytosis,[40] *Nts* ($\log_2FC = -0.409$, adj. $p = 0.0295$), neuropeptide receptor binding,[41] *Arrb2* ($\log_2FC = -0.313$, adj. $p = 0.0348$), a modulator of β-adrenergic and dopamine signaling,[42] and *Sorcs3* ($\log_2FC = -0.225$, adj. $p = 0.0232$), a regulator of long-term synaptic depression.[43] Those upregulated due to stress included: *Plxnd1* ($\log_2FC = 0.695$, adj. $p = 0.0263$), involved in synapse assembly,[44] *Drd2* ($\log_2FC = 0.650$, adj. $p = 0.0390$), a dopamine receptor,[45] *Unc13c* ($\log_2FC = 0.580$, adj. $p = 0.0147$), involved in glutamatergic transmission,[46] *Adra2c* ($\log_2FC = 0.530$, adj. $p = 0.0484$), an adrenergic receptor,[47] *Tgfa* ($\log_2FC = 0.459$, adj. $p = 0.0431$),[33] *Gabra4* ($\log_2FC = 0.455$, adj. $p = 0.0067$), a subunit of the GABA receptor,[48] *Camk2n1* ($\log_2FC = 0.413$, adj. $p = 0.0196$),[34] *Cplx2* ($\log_2FC = 0.380$, adj, $p = 0.0230$),[35] and *Gpr158* ($\log_2FC = 0.361$, adj. $p = 0.0431$), a GPCR implicated in depression.[49] Taken together, this suggests that stress causes major changes in synaptic signaling in the adBNST in males. A further list of selected DEGs of interest that are downregulated or upregulated due to stress, along with their $\log_2FC$, adjusted *p*-value, and functional relevance, can be found in Tables 3 and 4, respectively. A list of all stress-regulated genes can be found in Supplementary Table 4.

13652826, 2025, 8, Downloaded from https://onlinelibrary.wiley.com/doi/10.1111/jne.70041 by Benjamin Samuels - Rutgers University Libraries , Wiley Online Library on [07/11/2026]. See the Terms and Conditions (https://onlinelibrary.wiley.com/terms-and-conditions) on Wiley Online Library for rules of use; OA articles are governed by the applicable Creative Commons License

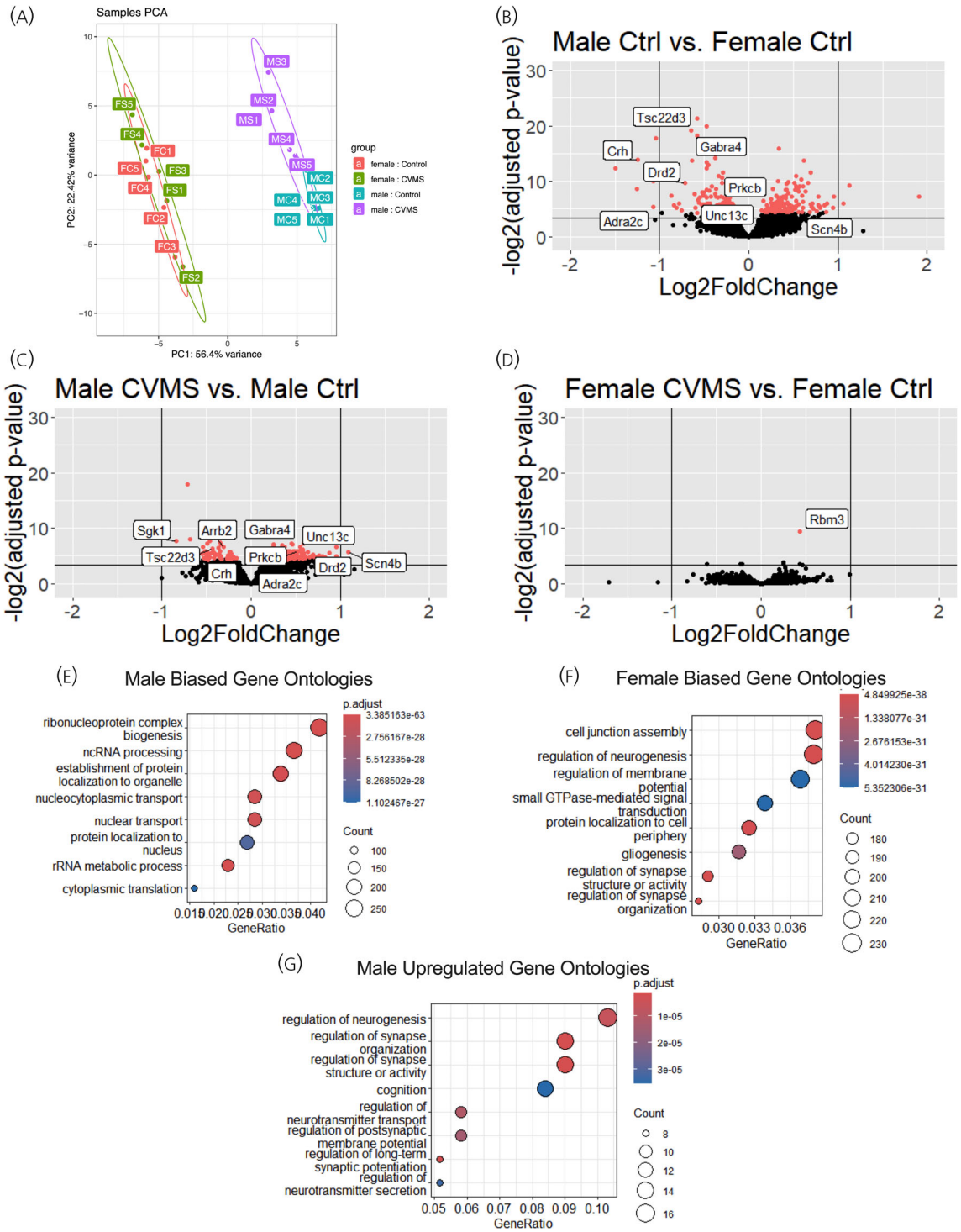


FIGURE 2 Bulk RNA-Sequencing of the anterodorsal bed nucleus of the stria terminalis. (A) Principal component analysis of all samples. (B) Volcano plot comparing control males and control females. A positive fold change represents a female-biased gene while a negative fold change represents a male-biased gene. (C, D) Volcano plots comparing control and stressed animals in (C) males and (D) females. A positive fold change represents an upregulation due to stress while a negative fold change represents a downregulation due to stress. (E, F) Gene ontology analyses comparing control males and control females, (E) pathways enriched in control males (F) pathways enriched in control females. (G) Gene ontology analysis comparing control males and stressed males showing pathways upregulated due to stress. A is analyzed by PCAexplorer; (B–D) are analyzed by DESeq2; and (E, F) are analyzed by enrichGO. Significant DEGS are highlighted in red in (B–D).

Comparing control males and females for gene ontology enrichment, pathways that were male biased were mostly related to RNA processing and protein localization (Figure 2E) whereas pathways upregulated in females are related to neuronal activity, such as neurogenesis and regulation of the synapse (Figure 2F). Comparing control males to stressed males, pathways that are upregulated due to stress

13652826, 2025, 8, Downloaded from https://onlinelibrary.wiley.com/doi/10.1111/jne.70041 by Benjamin Samuels - Rutgers University Libraries , Wiley Online Library on [07/11/2026]. See the Terms and Conditions (https://onlinelibrary.wiley.com/terms-and-conditions) on Wiley Online Library for rules of use; OA articles are governed by the applicable Creative Commons License

TABLE 1 Genes that are male-biased in the adBNST when comparing control males and control females. Genes are listed in order of the log_2 fold change. A full list of all male-biased genes can be found in Table S1.

Male-biased genes			
Gene	**Log_2 fold change**	**Adjusted *p*-value**	**Function**
Ddx3y	10.335414	2.25E-58	Highest male-biased fold change
Hcrtr1	1.075102	0.02403575	Receptor
Plekhf1	1.0685986	0.00092238	Cell signaling
Sgk1	1.0453092	4.45E-06	Synaptic signaling
Tac2	0.7833121	0.01666949	Receptor
Mc4r	0.7118213	0.00124686	Receptor
Tsc22d3	0.6430774	1.78E-06	Transcription factor
Crh	0.5717431	0.01086472	Neuropeptide
N4bp2	0.4978987	0.00402842	Neuronal excitability
Slc5a3	0.470757	9.80E-07	Ion channel
Prr5	0.4149862	0.00186334	Cell signaling
Fam126a	0.3768818	5.52E-05	Cell signaling
Mat2a	0.301764	0.00124686	Cell signaling
Insyn2a	0.2799577	0.02967483	Synaptic signaling
Irs2	0.2523133	0.00774428	Cell signaling
Dpysl2	0.2273524	0.00159526	Synaptic signaling
Gna13	0.1976531	0.02541766	Synaptic signaling

are mostly related to synaptic activity and neurotransmission (Figure 2G). There were no pathways that were significantly downregulated due to stress in males.

3.3 | Electrophysiology

3.3.1 | M-current

In examination of stress-induced changes in excitability in the adBNST from CRH-expressing neurons, we found no differences in the resting membrane potential between the experimental groups. The average RMP in CRH neurons in control males was −69.2 ± 2.2 mV, in stressed males, −69.0 ± 1.9 mV, in control females, −68.7 ± 1.9 mV, and in stressed females, −67.7 ± 2.3 mV (ns, Figure 3B). We also found no differences in the change in input resistance (Rin) due to XE-991, the KCNQ channel blocker. The average change in Rin in control males was −0.39 ± 0.18 pA, in stressed males, −0.38 ± 0.09 pA, in control females, −0.43 ± 0.11 pA, and in stressed females, −0.22 ± 0.14 pA (ns, Figure 3C).

As we have previously characterized the M-current in oval BNST (ovBNST) CRH neurons in male mice,[50] we next examined the M-current in CRH neurons across the sexes. We found that CRH neurons from males and females did not have significant differences in the strength of their M-currents in control conditions (not shown). However, we did find an effect of CVMS in the males, as we previously found,[50] but not in CRH neurons from female mice. XE-991 perfusion suppressed the M-current activity in control male mice [interaction effect (Voltage × XE-991): $F(9,126) = 5.728$, $p < 0.0001$; −75 mV: 0.0250; −50 mV: 0.0118; −45 mV: $p = 0.0028$; −40 mV: $p = 0.0029$; −35 mV: $p = 0.0017$; −30 mV: $p = 0.0131$] (Figure 3D). However, in stressed males, while they had a significant interaction effect, their current traces only differed at −75 mV [interaction effect (Voltage × XE-991): $F(9, 144) = 2.871$, $p = 0.0038$; −75 mV: $p = 0.0383$] (Figure 3E). The max peak, defined as the strength of the current at −35 mV, in CRH neurons from males was significantly decreased after exposure to XE-991 [main effect of XE-991: $F(1, 30) = 1.547$, $p = 0.0222$] (Figure 3F). However, the traces of the XE-991 sensitive current were significantly decreased in CRH neurons from stressed males in comparison to control males [interaction effect (Voltage × Treatment): $F(9,135) = 2.698$, $p < 0.0001$; −50 mV: $p = 0.0279$; −45 mV: $p = 0.0125$; −40 mV; $p = 0.0281$; −35 mV: $p = 0.0115$; −30 mV: $p = 0.0468$] (Figure 3G).

The M-current was suppressed by XE-991 perfusion in CRH neurons from both control and stressed female mice (Figure 3H, I). Max peak was trending reduced in both control and stressed groups after XE-991 perfusion [main effect of XE-991: $F(1, 30) = 4.112$, $p = 0.0515$], indicating that the M-current is active in these neurons. Further, CVMS did not alter the XE-991 sensitive current in CRH neurons from female mice.

3.3.2 | EPSCs

We next examined the influence of CVMS on EPSCs in both sexes. Previous studies in our lab suggest that CVMS augments EPSCs in male mice.[50] In the current study, CVMS did not change the frequency, amplitude, or charge of EPSCs in male mice. CRH neurons from control males in vehicle conditions exhibited an average of 159.4 ± 47.5 EPSC events, while in stressed males, CRH neurons

13652826, 2025, 8, Downloaded from https://onlinelibrary.wiley.com/doi/10.1111/jne.70041 by Benjamin Samuels - Rutgers University Libraries , Wiley Online Library on [07/11/2026]. See the Terms and Conditions (https://onlinelibrary.wiley.com/terms-and-conditions) on Wiley Online Library for rules of use; OA articles are governed by the applicable Creative Commons License

TABLE 2 Genes that are female-biased in the adBNST when comparing control males and control females. Genes are listed in order of the log2 fold change. A full list of all female-biased genes can be found in Table S2.

Female-biased genes			
Gene	**Log_2 fold change**	**Adjusted *p*-value**	**Function**
Xist	12.0753291	4.74E-247	Highest female-biased fold change
Scn4b	1.06144811	0.01592177	Ion channel
Unc13c	0.69298312	0.0003445	Synaptic signaling
Gsg1l	0.60262271	0.01313623	Synaptic signaling
Rgs7bp	0.56399579	0.00181925	Synaptic signaling
Tgfa	0.52973038	0.01129631	Growth factor
Pcp4	0.51704562	0.00270595	Synaptic signaling
Kcnab1	0.4574967	0.01979391	Ion channel
Dgkb	0.45423177	0.02057618	Synaptic signaling
Camk2n1	0.44342939	0.00457921	Synaptic signaling
Cacng3	0.42791418	0.04830886	Synaptic signaling
Pcsk2	0.41706433	0.00572449	Synaptic signaling
Gabra4	0.40890884	0.00790706	Receptor
Gpr158	0.39768693	0.01796807	Receptor
Spock3	0.38562695	0.00673688	Calcium regulation
Lrrtm3	0.36543401	0.01125902	Synaptic signaling
Cplx2	0.34982939	0.02967483	Synaptic signaling
Neto2	0.32994357	0.01532972	Synaptic signaling
Cdh8	0.32613862	0.00786683	Cellular adhesion
Anks1b	0.30290019	0.04046966	Synaptic signaling
Adcy1	0.29883662	0.01387116	Synaptic signaling
Cacnb4	0.28553624	0.04816953	Ion channel
Cplx1	0.28103691	0.04227382	Synaptic signaling
Tmem132b	0.26624608	0.00249415	Receptor
Comt	0.21502622	0.04332065	Synaptic signaling
Gpm6b	0.19125504	0.03356488	Synaptic signaling
Slc1a2	0.18134176	0.03972835	Transporter

exhibited an average of 145 ± 43.8 EPSCs (ns, Figure 4B). In the same neurons, the average EPSC amplitude was −8.65 ± 1.0 pA from control males, and the average EPSC amplitude was −9.8 ± 1.0 pA in neurons from stressed males (ns, Figure 4C). The charge of EPSCs in neurons from control males was an average Q of −82.7 ± 12.6 pA*ms, and in neurons from stressed males, an average of −71.2 ± 15.3 pA*ms (ns, Figure 4D).

After the initial recording of EPSCs, we perfused each CRH neuron with Stressin 1 to determine if CRH acts in a feedback loop within the adBNST CRH neuronal population, either in an autocrine or paracrine fashion. After perfusion with Stressin I, the frequency of EPSCs in CRH neurons from control males was an average of 131.5 ± 42.5 events and from stressed males was an average of 115 ± 21.7 events (ns, Figure 4B). The amplitude of EPSCs in CRH neurons from control males was an average of −9.0 ± 0.8 pA, whereas in CRH neurons from stressed males, it was an average of −10.3 ± 0.9 pA (ns) (Figure 4C). The average charge (Q) of EPSCs from control males was −68.3 ± 2.9 pA*ms and from stressed males was −78.0 ± 12.6 pA*ms (ns, Figure 4D).

CRH neurons from female mice exhibited differences in the amplitude of their EPSCs due to stress. The frequency of EPSCs in CRH neurons from control females in vehicle conditions was an average of 73.8 ± 29.5 events, and from stressed females, was an average of 75.0 ± 11.2 EPSCs (ns, Figure 4E). The amplitude of EPSCS in CRH neurons from control females in vehicle was an average of −13.7 ± 1.6 pA, whereas from stressed females, was an average of −8.5 ± 1.0 pA [main effect of stress: $F(1, 28) = 12.77$, $p = 0.0013$] (Figure 4F). The charge (Q) of EPSCS in CRH neurons from control females in vehicle was an average of −81.7 ± 13.3 pA*ms, and in neurons from stressed females, was an average of −62.7 ± 5.7 pA*ms (Figure 4G).

After perfusion with Stressin I, EPSC frequency in CRH neurons from control females was 121.1 ± 33.7 and in CRH neurons from stressed females was 87.8 EPSCs ±16.6 (ns, Figure 4E). EPSC amplitude was −13.1 ± 1.8 pA in CRH neurons from control females and − 8.6 ± 1.0 pA from stressed females [main effect of stress: $F(1, 28) = 12.77$, $p = 0.0013$] (Figure 4F). The average Q was −72.4 ± 12.6 pA*ms in CRH neurons from control females and − 61.9 ± 4.9 pA*ms in CRH neurons from stressed females (ns, Figure 4G).

13652826, 2025, 8, Downloaded from https://onlinelibrary.wiley.com/doi/10.1111/jne.70041 by Benjamin Samuels - Rutgers University Libraries , Wiley Online Library on [07/11/2026]. See the Terms and Conditions (https://onlinelibrary.wiley.com/terms-and-conditions) on Wiley Online Library for rules of use; OA articles are governed by the applicable Creative Commons License

TABLE 3 Selected genes that are downregulated by stress in the adBNST in males. Genes are listed in order of the log2 fold change. A full list of all genes regulated by stress in males can be found in Table S3.

Male stress downregulated			
Gene	**Log_2 fold change**	**Adjusted *p*-value**	**Function**
Sgk1	−0.8415739	0.00501306	Most downregulated gene
Slc1a6	−0.5518564	0.02320938	Transporter
Akap12	−0.5109548	0.01745418	Synaptic signaling
Crh	−0.4851822	0.04204631	Neuropeptide
Tsc22d3	−0.4394077	0.01335128	Transcription factor
Vamp1	−0.4242631	0.01961082	Synaptic signaling
Nts	−0.4087929	0.0294921	Neuropeptide
Slc5a3	−0.3474649	0.00607686	Ion channel
Otof	−0.3466157	0.04284925	Synaptic signaling
Prr5	−0.3443065	0.01854398	Cell signaling
Alk	−0.3421647	0.03482863	Synaptic signaling
Arrb2	−0.3132115	0.01075937	Synaptic signaling
Epha5	−0.2674514	0.04311296	Receptor
Grk3	−0.2649624	0.04374024	Synaptic signaling
Sema4a	−0.2401795	0.04735542	Synaptic signaling
Sorcs3	−0.22523	0.02320938	Synaptic signaling
Dpysl2	−0.1670872	0.04284925	Synaptic signaling

When comparing males and females, we do see differences in the amplitude of the EPSCs. Both in vehicle and Stressin I, EPSC amplitude was significantly lower in CRH neurons from females with a main effect of sex ($F(1,24) = 9.587$, $p = 0.0049$, Figure 4G). We do not observe differences in the stressed animals, suggesting that CVMS causes the female CRH neurons to behave similarly to CRH neurons in males, though this cannot be confirmed (Figure 4H). This suggestion is further supported by the interaction effect in Figure 4I, which indicates that the EPSCs in CRH neurons from females and males are responding differently to stress [$F(1,26) = 7.114$, $p = 0.0130$], which appears to be mainly driven by the stronger amplitude of EPSCs in the control females (pairwise comparison to control males: $p = 0.0398$; pairwise comparison to stressed females: $p = 0.0180$).

4 | DISCUSSION

Our previous research using CVMS suggested that the transcriptome of the adBNST was not affected by stress, nor did it affect the M-current in NPY neurons of the adBNST.[18] This seemingly contradicted our hypothesis that the BNST was a major processing center for chronic stress. However, these current findings necessitate further research into the BNST and its relations to stress signaling, mood disorders, and sex variability. In contrast to our past research, this study suggests that there are transient changes in the transcriptome due to stress in males but not females, suggesting that adBNST neurons and their signaling properties are altered by chronic stress, but in mechanisms that vary across the sexes.

We found an abundance of genes that were differentially expressed between males and females and regulated by stress in the males. Interestingly, we found no such differences in the females, already suggesting that stress is affecting this area differently in males and females. The lack of response to CVMS in females also suggests that the adBNST is an important mediator of stress in males but not in females and that the major central stress-regulating region in females may be elsewhere. This hypothesis is further supported by the fact that presynaptic EPSCs were affected by stress in the females but not in the males.

Alternatively, this data could suggest that CVMS is not effective on the adBNST transcriptome or CRH neurophysiology in females; although our previous publication found that females were sensitive behaviorally to the same CVMS paradigm, which was dependent on the estrous cycles.[18] As we did not see differences due to stress in final cumulative BW gain or adBNST transcriptome, this suggests there may be a resistance to CVMS. Historically, literature has been contradictory in how sex relates to sensitivity of CMVS in mice.[51] This issue is further compounded by the limited research of CVMS in mice compared to rats, the limited research of CVMS in females, and potential strain differences, which also show differing sensitivities to stress.[52] Further research should control for the estrous stage in the RNA-sequencing, along with electrophysiology tests in differing estrous stages to test this. We believe this, along with our data showing increased EPSC strength in stressed females, suggests the need for further research on the effectiveness of CVMS in females.

In terms of sex differences in the transcriptome of the adBNST, the gene ontology data shows that male-biased genes are related to transcriptional regulation while female-biased genes are related to synaptic processing, suggesting that the BNST in females may be more plastic, especially at their synapse. For example, female-biased genes include *Gsg1l* and *Cacng3*, which both regulate AMPA signaling.

13652826, 2025, 8, Downloaded from https://onlinelibrary.wiley.com/doi/10.1111/jne.70041 by Benjamin Samuels - Rutgers University Libraries , Wiley Online Library on [07/11/2026]. See the Terms and Conditions (https://onlinelibrary.wiley.com/terms-and-conditions) on Wiley Online Library for rules of use; OA articles are governed by the applicable Creative Commons License

TABLE 4 Selected genes that are upregulated by stress in the adBNST in males. Genes are listed in order of the log2 fold change. A full list of all genes regulated by stress in males can be found in Table S3.

Male stress upregulated			
Gene	**Log_2 fold change**	**Adjusted *p*-value**	**Function**
Scn4b	1.08954915	0.01961082	Most upregulated gene
Rasd2	0.87684047	0.02308458	Synaptic signaling
Ppp1r1b	0.7098293	0.03707918	Cell signaling
Plxnd1	0.69541227	0.02628802	Synaptic signaling
Itpr1	0.6703348	0.03462583	Receptor
Drd2	0.65004132	0.03902923	Receptor
Ano2	0.61227969	0.00607686	Ion channel
Gng7	0.59981204	0.03850164	Receptor
Musk	0.5834368	0.02217479	Synaptic signaling
Unc13c	0.58046104	0.01465707	Synaptic signaling
Slc18a3	0.57407102	0.0426947	Transporter
Adra2c	0.52976636	0.04836964	Receptor
Penk	0.50832335	0.03386401	Neuropeptide
Ddn	0.50724373	0.01961082	Synaptic signaling
Rgs7bp	0.50103361	0.01817878	Synaptic signaling
Dapp1	0.48901824	0.01854398	Cell signaling
Kcnab1	0.48442864	0.01961082	Ion channel
Lzts3	0.4828807	0.03043355	Synaptic signaling
Kcna4	0.47734195	0.04524505	Ion channel
Tgfa	0.45877183	0.04311296	Growth factor
Gabra4	0.45498929	0.006678	Receptor
Filip1	0.45307766	0.03310177	Synaptic signaling
Mctp1	0.43760904	0.04204631	Synaptic signaling
Epha7	0.42772808	0.04204631	Receptor
Camk2n1	0.41345675	0.0195909	Synaptic signaling
Pcsk2	0.40659244	0.01681495	Protein modification
Shank3	0.39997231	0.04311296	Synaptic signaling
Cplx2	0.38001612	0.02296941	Synaptic signaling
Gpr158	0.36139748	0.04311296	Receptor
Spock3	0.34781457	0.02857924	Calcium regulation
Igsf11	0.29617933	0.03138945	Synaptic signaling
Adcy1	0.26192307	0.04311296	Synaptic signaling
Tmem123b	0.25428606	0.01075937	Receptor
Frmpd4	0.23296982	0.01681495	Synaptic signaling

Gsg1l acts to negatively regulate AMPA receptors by slowing the deactivation and desensitization of AMPA receptors.[53] *Cacng3* is a transmembrane AMPA regulatory protein (TARP) which is a family of proteins that positively regulate AMPA receptors. TARPs act by promoting AMPA receptor trafficking to the synapse and stabilization in the postsynaptic density.[54] With the transcripts of both negatively and positively regulating proteins being female-biased, it suggests that the neurons in the female adBNST are more primed for synaptic plasticity than males. This hypothesis is further supported by other genes involved in synaptic plasticity and axonogenesis, such as *Anks2b* and *Pcp4*, which are female-biased.

However, while the female adBNST may be primed for synaptic plasticity, the data suggest that only the transcriptome of the male adBNST is sensitive to stress. Of the genes that are regulated by stress, many are related to synaptic signaling, as evidenced by the gene ontologies and specific genes. For example, many downregulated genes are signaling molecules, their receptors, or regulators of their receptors, such as *Crh*, corticotropin-releasing hormone, *Slc1a6*, a glutamate transporter,[39] and *Arrb2*, an inhibitor of arrestin receptors.[42] Additionally, some are related to synaptic maintenance and signaling in general, such as *Vamp1*, which is involved in synaptic vesicle exocytosis,[40] *Otof*, which is involved in synaptic vesicle priming,[55] and

13652826, 2025, 8, Downloaded from https://onlinelibrary.wiley.com/doi/10.1111/jne.70041 by Benjamin Samuels - Rutgers University Libraries , Wiley Online Library on [07/11/2026]. See the Terms and Conditions (https://onlinelibrary.wiley.com/terms-and-conditions) on Wiley Online Library for rules of use; OA articles are governed by the applicable Creative Commons License

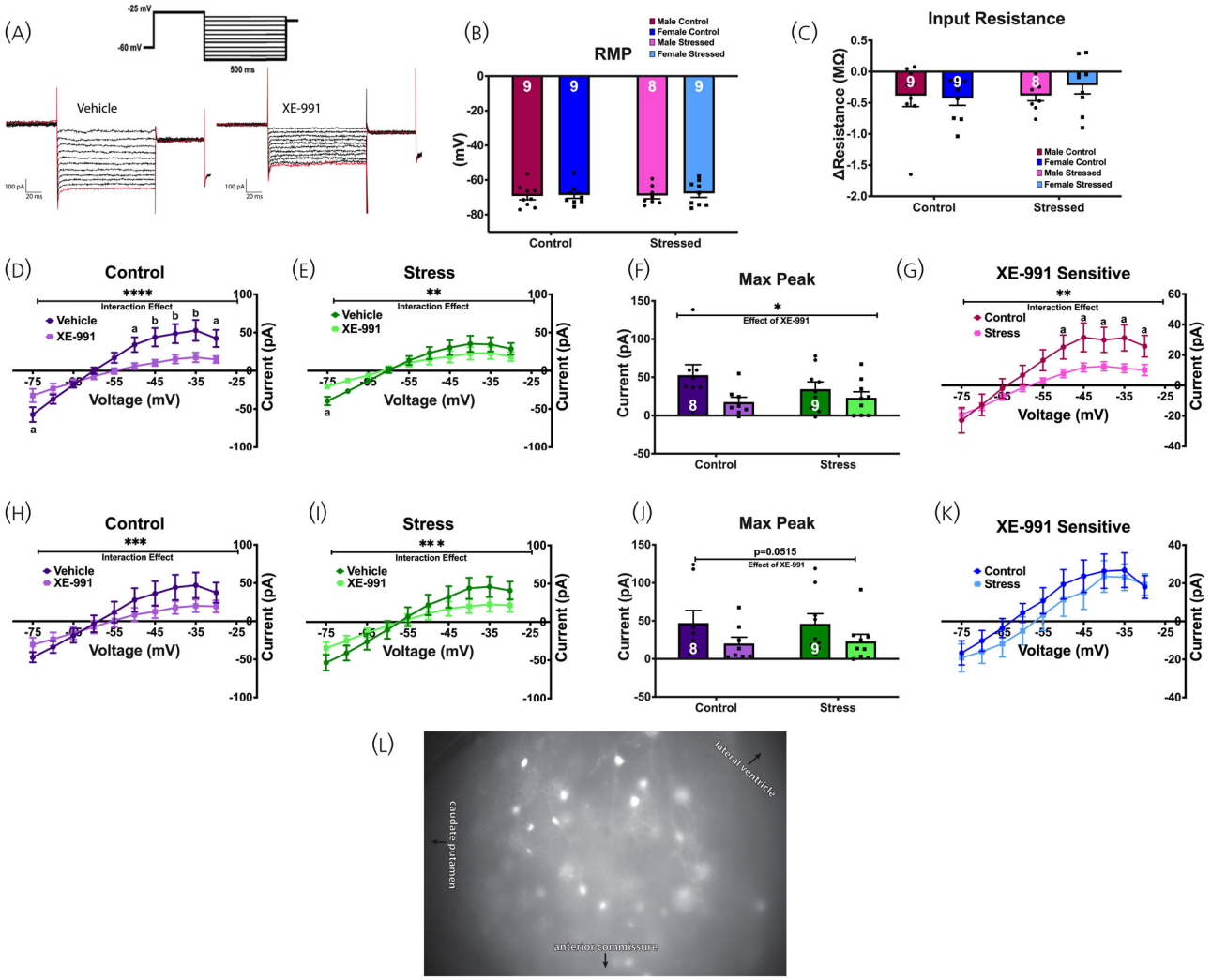


FIGURE 3 Recordings of M-current activity of BNST corticotropin-releasing factor-expressing neurons from stressed and non-stressed mice. (A) M-current protocol and representative traces. (B) Resting membrane potential of the neurons. (C) Change in input resistance after perfusion with XE-991. I–V plots from −75 to −30 mV after XE-991 perfusion in (D) Control male mice and (E) CVMS-exposed male mice. (F) Current at max peak in male mice. (G) I–V plot of XE-991 sensitive current in male mice. (H–K) Control and CVMS-exposed female mice. (L) Representative image of CRF+ neurons fluorescing in the adBNST. Data are presented as mean +/− SEM. Lower-case letters represent significant pairwise comparisons in the current traces. Asterisks with bracketed lines represent pairwise comparisons in the bar graphs. Asterisks with capped lines represent significant main effects with the comparison written below the capped line. ($a = 0.05–0.01$) (** = 0.01–0.001, **** < 0.0001).

Dpysl2, which is involved in axon growth.[56] Upregulated genes also follow a similar pattern of affecting synaptic transmission and catecholamine signaling. Examples include *Drd2*, a dopamine receptor,[45] *Adra2c*, an adrenergic receptor,[47] and *Camk2n1* and *Igsf11*, which are both involved in long-term potentiation.[34,57] This suggests that chronic stress causes major changes in the regulation of the synapse in the adBNST of males.

However, one must ask if this is truly a reflection of chronic stress or acute stress. Our previous publication showed no transcriptomic differences due to CVMS 18 h post-stress[18] but in the current study, we found over 200 DEGs in the males 1 h post-stress. However, the transcriptional effects of chronic stress did lead to sustained (17–24 h post-stress) neurophysiological outcomes in males. It is possible that our results are due specifically to chronic stress and the transcriptome is so transient that differences are lost quickly when there is no stress, or it could be equally possible that this is due to the mild acute stress. One study using chronic mild stress paradigms found sustained differences in the nucleus accumbens 24 h after the last stressor.[58] Two other studies found stress-sensitive genes in the amygdala, hippocampus, and hypothalamus after chronic stress but waited to collect tissue until after multiple days of behavior testing.[59,60] Comparisons between chronic stress studies can be difficult though, as the chronic stress paradigms often differ significantly between labs, and the transcriptome of different brain regions or cell types may have differing reaction times to stress. Additionally, Karisetty et al. and Yang et al. used behavior tests to ensure the mice expressed stress-induced behavioral changes before transcriptomic analysis, which we did not do, further complicating comparisons. Further experiments may be necessary, such as measuring the adBNST transcriptome in samples collected 1 h after the

13652826, 2025, 8, Downloaded from https://onlinelibrary.wiley.com/doi/10.1111/jne.70041 by Benjamin Samuels - Rutgers University Libraries , Wiley Online Library on [07/11/2026]. See the Terms and Conditions (https://onlinelibrary.wiley.com/terms-and-conditions) on Wiley Online Library for rules of use; OA articles are governed by the applicable Creative Commons License

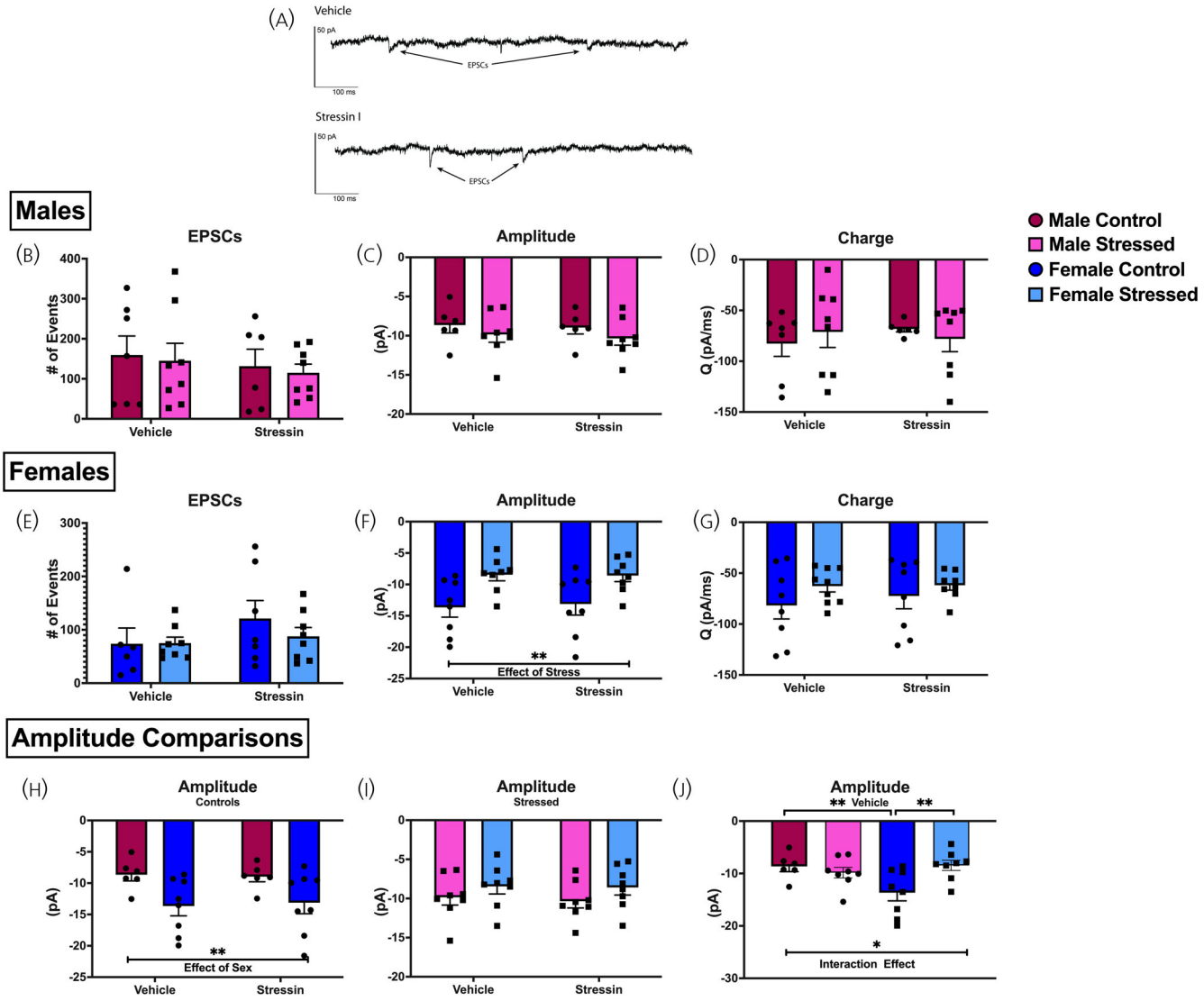


FIGURE 4 Recordings of EPSCs in CRF-expressing neurons of the adBNST from control and stressed mice. (A) Representative traces of current recordings for EPSCs in vehicle and after exposure to Stressin I. Number of EPSCs detected in a 5-minute voltage-clamp recording in vehicle and after exposure to Stressin I in (B) male and (E) female mice. Average amplitude of EPSCs detected in (C) male and (F) female mice. Average charge of EPSCs detected in (D) male and (G) female mice. (H) Comparison of average amplitude in males and females in control mice. (I) Comparison of average amplitude in male and female mice in stressed mice. (J) Comparison of average amplitude between males and females and control and stressed when cells are in vehicle conditions. Data is presented as mean +/− SEM. Analyzed via two-way ANOVA. Asterisks with bracketed lines represent significant pairwise comparisons. Asterisks with capped lines represent significant main effects with the comparison written below the capped line. (* = 0.05–0.01, ** = 0.01–0.001).

typical last stressor (1 h wet bedding) without the chronic stress paradigm.

As the transcriptome data suggest that only the male adBNST is sensitive to stress, this is also supported by chronic stress affecting the M-current in males but not females. Chronic stress significantly decreased the strength of the M-current in males, supporting our previously published findings.[19] The M-current is an intrinsic property of the neuron and is produced by voltage-gated K^+ channels, the KCNQ channels. This current is inhibitory and is significant as it is one of the few currents that is active at physiologically relevant voltages and, as such, has a strong influence on the resting membrane potential of the cell.[24] This weakening of the M-current by stress infers that these neurons are more likely to fire, possibly leading to increased signaling by the BNST and increased release of CRH or GABA. This further supports our hypothesis that CVMS directly affects the adBNST neurons in males but not females.

The results in females suggest there may be different areas of the brain that are more important for chronic stress processing. As the transcriptome data suggests, the adBNST in females is not sensitive to CVMS as the only gene affected by it was *Rbm3*, a gene that is

13652826, 2025, 8, Downloaded from https://onlinelibrary.wiley.com/doi/10.1111/jne.70041 by Benjamin Samuels - Rutgers University Libraries , Wiley Online Library on [07/11/2026]. See the Terms and Conditions (https://onlinelibrary.wiley.com/terms-and-conditions) on Wiley Online Library for rules of use; OA articles are governed by the applicable Creative Commons License

related to cellular stress.[61] Additionally, the electrophysiology data supports examining other regions critical to stress or steroid hormone signaling as we saw significant differences in the females to EPSCs. EPSCs, being an extrinsic property, show that neurons other than the CRF-expressing adBNST neurons are possibly being affected by stress, and we are seeing that downstream through their synaptic transmission.[62] However, it is important to recognize that the strength of EPSCs can be modulated either in the pre-synapse or in the post-synapse. In the pre-synapse, EPSC strength can be modulated by the loading of vesicles,[63] the docking position of vesicles,[64] and the number of vesicles primed for release[65]; whereas the post-synapse can modulate the strength of EPSCs by altering the number of receptors at the synapse, modulating the effects of those receptors, and increasing dendritic arborization.[66] While both sites can affect the strength of EPSCs, computational neuroscience suggests that the pre-synapse has the greater control of the strength of EPSCs.[66–68] This has also been supported experimentally, which showed that mature neurons typically use pre-synaptic methods to modulate EPSC strength while younger neurons utilize post-synaptic methods.[69] There are limitations to these studies, though, as they have been done almost exclusively in hippocampal neurons or at the neuromuscular junction as these synapses are well-characterized. It is possible that, in the BNST, post-synaptic modulation is more important; however, since we do not see any changes in receptors or related proteins in the RNA-sequencing data, we infer that this change in females is related to the pre-synapse. More research should be conducted to confirm this, though. Furthermore, our data is supported by the lack of response to CRH receptor activation either in the M-current or EPSCs, demonstrating that adBNST CRH neurons do not respond to other CRH neurons. However, this does not preclude other types of neurons in the BNST causing these changes. One potential site is the posterior BNST, which expresses high levels of steroid receptors and sends projections to the adBNST.[6,70]

Our data suggests that chronic stress is processed differently in the brains of male and female mice. However, surprisingly, it also suggests that they are not only processed differently but potentially processed by separate areas of the brain. Further research is needed to elucidate which other areas are important and how these differences in signaling are related to the development of mood disorders. Additionally, this experiment only used one type of stress paradigm. It is well known that different types of stress are processed differently; thus, further studies are also needed to be done to determine how the processing of psychosocial stress may differ from physiological stress, for example.

AUTHOR CONTRIBUTIONS

Thomas J. Degroat: Writing – original draft; methodology; data curation; formal analysis; investigation; conceptualization. **Sarah Paladino:** Investigation; data curation; formal analysis. **Benjamin A. Samuels:** Conceptualization; funding acquisition; writing – review and editing. **Troy A. Roepke:** Writing – review and editing; conceptualization; funding acquisition; supervision; resources; project administration.

ACKNOWLEDGMENTS

This research is funded by NIH/NIMH R01MH123544 (T. A. R. and B. S). We would also like to thank Dr. Katherine Denney for their assistance with RNA Sequencing analysis.

CONFLICT OF INTEREST STATEMENT

The authors declare no conflicts of interest.

PEER REVIEW

The peer review history for this article is available at https://www.webofscience.com/api/gateway/wos/peer-review/10.1111/jne.70041.

DATA AVAILABILITY STATEMENT

The data that support the findings of this study are openly available in Gene Expression Omnibus at http://ncbi.nlm.nih.gov/geo, reference number GSE281507.

ORCID

Troy A. Roepke https://orcid.org/0000-0001-5426-2266

REFERENCES

1. Herman JP, Ostrander MM, Mueller NK, Figueiredo H. Limbic system mechanisms of stress regulation: hypothalamo-pituitary-adrenocortical axis. *Prog Neuropsychopharmacol Biol Psychiatry*. 2005;29(8):1201-1213. doi:10.1016/j.pnpbp.2005.08.006
2. Poe GR, Foote S, Eschenko O, et al. Locus coeruleus: a new look at the blue spot. *Nat Rev Neurosci*. 2020;21(11):644-659. doi:10.1038/s41583-020-0360-9
3. Bonaz B, Rivest S. Effect of a chronic stress on CRF neuronal activity and expression of its type 1 receptor in the rat brain. *Am J Physiol*. 1998;275(5):R1438-R1449. doi:10.1152/ajpregu.1998.275.5.R1438
4. Chappell P, Smith M, Kilts C, et al. Alterations in corticotropin-releasing factor-like immunoreactivity in discrete rat brain regions after acute and chronic stress. *J Neurosci*. 1986;6(10):2908-2914. doi:10.1523/jneurosci.06-10-02908.1986
5. Hellriegel ET, D'Mello AP. The effect of acute, chronic and chronic intermittent stress on the central noradrenergic system. *Pharmacol Biochem Behav*. 1997;57(1):207-214. doi:10.1016/S0091-3057(96)00341-3
6. Becker JAJ, Befort K, Blad C, et al. Transcriptome analysis identifies genes with enriched expression in the mouse central extended amygdala. *Neuroscience*. 2008;156(4):950-965. doi:10.1016/j.neuroscience.2008.07.070
7. Perez-Villalba A, Teruel-Martí V, Ruiz-Torner A, Olucha-Bordonau F. The effect of long context exposure on cued conditioning and c-fos expression in the rat forebrain. *Behav Brain Res*. 2005;161(2):263-275. doi:10.1016/j.bbr.2005.02.028
8. Hammack SE, Todd TP, Kocho-Schellenberg M, Bouton ME. Role of the bed nucleus of the stria terminalis in the acquisition of contextual fear at long or short context-shock intervals. *Behav Neurosci*. 2015;129(5):673-678. doi:10.1037/bne0000088
9. Waddell J, Morris RW, Bouton ME. Effects of bed nucleus of the stria terminalis lesions on conditioned anxiety: aversive conditioning with long-duration conditional stimuli and reinstatement of extinguished fear. *Behav Neurosci*. 2006;120(2):324-336. doi:10.1037/0735-7044.120.2.324
10. Vyas A, Bernal S, Chattarji S. Effects of chronic stress on dendritic arborization in the central and extended amygdala. *Brain Res*. 2003;965(1–2):290-294. doi:10.1016/s0006-8993(02)04162-8

13652826, 2025, 8, Downloaded from https://onlinelibrary.wiley.com/doi/10.1111/jne.70041 by Benjamin Samuels - Rutgers University Libraries , Wiley Online Library on [07/11/2026]. See the Terms and Conditions (https://onlinelibrary.wiley.com/terms-and-conditions) on Wiley Online Library for rules of use; OA articles are governed by the applicable Creative Commons License

11. Conrad KL, Louderback KM, Gessner CP, Winder DG. Stress-induced alterations in anxiety-like behavior and adaptations in plasticity in the bed nucleus of the stria terminalis. *Physiol Behav*. 2011;104(2):248-256. doi:10.1016/j.physbeh.2011.03.001
12. Daniel SE, Menigoz A, Guo J, Ryan SJ, Seth S, Rainnie DG. Chronic stress induces cell type-selective transcriptomic and electrophysiological changes in the bed nucleus of the stria terminalis. *Neuropharmacology*. 2019;150:80-90. doi:10.1016/j.neuropharm.2019.03.013
13. Willner P, Towell A, Sampson D, Sophokleous S, Muscat R. Reduction of sucrose preference by chronic unpredictable mild stress, and its restoration by a tricyclic antidepressant. *Psychopharmacology (Berl)*. 1987;93(3):358-364. doi:10.1007/bf00187257
14. Farhan M, Haleem DJ. Anxiolytic profile of fluoxetine as monitored following repeated administration in animal rat model of chronic mild stress. *Saudi Pharmaceutical Journal*. 2016;24(5):571-578. doi:10.1016/j.jsps.2015.03.006
15. Kompagne H, Bárdos G, Szénási G, Gacsályi I, Hársing LG, Lévay G. Chronic mild stress generates clear depressive but ambiguous anxiety-like behaviour in rats. *Behav Brain Res*. 2008;193(2):311-314. doi:10.1016/j.bbr.2008.06.008
16. Papp M, Gruca P, Lason-Tyburkiewicz M, Adham N, Kiss B, Gyertyán I. Attenuation of anhedonia by cariprazine in the chronic mild stress model of depression. *Behav Pharmacol*. 2014;25(5 and 6):567-574.
17. Wiborg O. Chronic mild stress for modeling anhedonia. *Cell Tissue Res*. 2013;354(1):155-169. doi:10.1007/s00441-013-1664-0
18. Degroat TJ, Wiersielis K, Denney K, et al. Chronic stress and its effects on behavior, RNA expression of the bed nucleus of the stria terminalis, and the M-current of NPY neurons. *Psychoneuroendocrinology*. 2024;161:106920. doi:10.1016/j.psyneuen.2023.106920
19. Hu P, Liu J, Maita I, et al. Chronic stress induces maladaptive behaviors by activating corticotropin-releasing hormone signaling in the mouse oval bed nucleus of the stria terminalis. *J Neurosci*. 2020a;40(12):2410-2419. doi:10.1523/jneurosci.2410-19.2020
20. Bromet E, Andrade LH, Hwang I, et al. Cross-national epidemiology of DSM-IV major depressive episode. *BMC med*. 2011;9(1):90. doi:10.1186/1741-7015-9-90
21. Hu P, Liu J, Yasrebi A, et al. Gq protein-coupled membrane-initiated estrogen signaling rapidly excites corticotropin-releasing hormone neurons in the hypothalamic paraventricular nucleus in female mice. *Endocrinology*. 2016;157(9):3604-3620. doi:10.1210/en.2016-1191
22. Brown DA, Adams PR. Muscarinic suppression of a novel voltage-sensitive K+ current in a vertebrate neurone. *Nature*. 1980;283(5748):673-676. doi:10.1038/283673a0
23. Robbins J. KCNQ potassium channels: physiology, pathophysiology, and pharmacology. *Pharmacol Ther*. 2001;90(1):1-19. doi:10.1016/S0163-7258(01)00116-4
24. Marrion NV. Control of M-current. *Annu Rev Physiol*. 1997;59:483-504. doi:10.1146/annurev.physiol.59.1.483
25. Scott MM, Marcus JN, Pettersen A, et al. Hcrtr1 and 2 signaling differentially regulates depression-like behaviors. *Behav Brain Res*. 2011;222:289-294. doi:10.1016/j.bbr.2011.02.044
26. Lang F, Strutz-Seebohm N, Seebohm G, Lang UE. Significance of SGK1 in the regulation of neuronal function. *J Physiol*. 2010;588(Pt 18):3349-3354. doi:10.1113/jphysiol.2010.190926
27. Al Abed AS, Reynolds NJ, Dehorter N. A second wave for the neurokinin Tac2 pathway in brain research. *Biol Psychiatry*. 2021;90(3):156-164. doi:10.1016/j.biopsych.2021.02.016
28. Tao YX. The melanocortin-4 receptor: physiology, pharmacology, and pathophysiology. *Endocr Rev*. 2010;31(4):506-543. doi:10.1210/er.2009-0037
29. Krueger-Burg D, Papadopoulos T, Brose N. Organizers of inhibitory synapses come of age. *Curr Opin Neurobiol*. 2017;45:66-77. doi:10.1016/j.conb.2017.04.003
30. Yamaguchi Y, Katoh H, Yasui H, Aoki J, Nakamura K, Negishi M. Gα12 and Gα13 inhibit Ca2+ -dependent exocytosis through rho/-rho-associated kinase-dependent pathway. *J Neurochem*. 2000;75(2):708-717. doi:10.1046/j.1471-4159.2000.0750708.x
31. Gu X, Mao X, Lussier MP, et al. GSG1L suppresses AMPA receptor-mediated synaptic transmission and uniquely modulates AMPA receptor kinetics in hippocampal neurons. *Nat Commun*. 2016;7(1):10873. doi:10.1038/ncomms10873
32. Milstein AD, Nicoll RA. Regulation of AMPA receptor gating and pharmacology by TARP auxiliary subunits. *Trends Pharmacol Sci*. 2008;29(7):333-339. doi:10.1016/j.tips.2008.04.004
33. Jun Ma Y, Junier M-P, Costa ME, Ojeda SR. Transforming growth factor-α gene expression in the hypothalamus is developmentally regulated and linked to sexual maturation. *Neuron*. 1992;9(4):657-670. doi:10.1016/0896-6273(92)90029-D
34. Astudillo D, Karmelic D, Casas BS, Otmakhov N, Palma V, Sanhueza M. CaMKII inhibitor 1 (CaMK2N1) mRNA is upregulated following LTP induction in hippocampal slices. *Synapse*. 2020;74(10):e22158. doi:10.1002/syn.22158
35. Yoon T-Y, Lu X, Diao J, Lee S-M, Ha T, Shin Y-K. Complexin and Ca2+ stimulate SNARE-mediated membrane fusion. *Nat Struct Mol Biol*. 2008;15(7):707-713. doi:10.1038/nsmb.1446
36. Younis RM, Taylor RM, Beardsley PM, McClay JL. The ANKS1B gene and its associated phenotypes: focus on CNS drug response. *Pharmacogenomics*. 2019;20(9):669-684. doi:10.2217/pgs-2019-0015
37. Harrison PJ, Tunbridge EM. Catechol-O-methyltransferase (COMT): a gene contributing to sex differences in brain function, and to sexual dimorphism in the predisposition to psychiatric disorders. *Neuropsychopharmacology*. 2008;33(13):3037-3045. doi:10.1038/sj.npp.1301543
38. Bjørnsen LP, Hadera MG, Zhou Y, Danbolt NC, Sonnewald U. The GLT-1 (EAAT2; slc1a2) glutamate transporter is essential for glutamate homeostasis in the neocortex of the mouse. *J Neurochem*. 2014;128(5):641-649. doi:10.1111/jnc.12509
39. Gegelashvili G, Dehnes Y, Danbolt NC, Schousboe A. The high-affinity glutamate transporters GLT1, GLAST, and EAAT4 are regulated via different signalling mechanisms. *Neurochem Int*. 2000;37(2):163-170. doi:10.1016/S0197-0186(00)00019-X
40. Liu Y, Sugiura Y, Lin W. The role of Synaptobrevin1/VAMP1 in Ca2+−triggered neurotransmitter release at the mouse neuromuscular junction. *J Physiol*. 2011;589(7):1603-1618. doi:10.1113/jphysiol.2010.201939
41. Mustain WC, Rychahou PG, Evers BM. The role of neurotensin in physiologic and pathologic processes. *Curr Opin Endocrinol Diabetes Obes*. 2011;18(1):75-82. doi:10.1097/MED.0b013e3283419052
42. Beaulieu J-M, Sotnikova TD, Marion S, Lefkowitz RJ, Gainetdinov RR, Caron MG. An Akt/β-Arrestin 2/PP2A signaling complex mediates dopaminergic neurotransmission and behavior. *Cell*. 2005;122(2):261-273. doi:10.1016/j.cell.2005.05.012
43. Breiderhoff T, Christiansen GB, Pallesen LT, et al. Sortilin-related receptor SORCS3 is a postsynaptic modulator of synaptic depression and fear extinction. *PLoS One*. 2013;8(9):e75006. doi:10.1371/journal.pone.0075006
44. Wang F, Eagleson KL, Levitt P. Positive regulation of neocortical synapse formation by the plexin-D1 receptor. *Brain Res*. 2015;1616:157-165. doi:10.1016/j.brainres.2015.05.005
45. Noble EP. The DRD2 gene in psychiatric and neurological disorders and its phenotypes. *Pharmacogenomics*. 2000;1(3):309-333. doi:10.1517/14622416.1.3.309
46. Padmanarayana M, Liu H, Michelassi F, et al. A unique C2 domain at the C terminus of Munc13 promotes synaptic vesicle priming. *Proc Natl Acad Sci U S A*. 2021;118(11):1-12. doi:10.1073/pnas.2016276118
47. Bylund DB. Subtypes of alpha 1- and alpha 2-adrenergic receptors. *FASEB J*. 1992;6(3):832-839. doi:10.1096/fasebj.6.3.1346768

13652826, 2025, 8, Downloaded from https://onlinelibrary.wiley.com/doi/10.1111/jne.70041 by Benjamin Samuels - Rutgers University Libraries , Wiley Online Library on [07/11/2026]. See the Terms and Conditions (https://onlinelibrary.wiley.com/terms-and-conditions) on Wiley Online Library for rules of use; OA articles are governed by the applicable Creative Commons License

48. Mulligan MK, Wang X, Adler AL, Mozhui K, Lu L, Williams RW. Complex control of GABA(a) receptor subunit mRNA expression: variation, covariation, and genetic regulation. *PLoS One*. 2012;7(4):e34586. doi:10.1371/journal.pone.0034586
49. Sutton LP, Orlandi C, Song C, et al. Orphan receptor GPR158 controls stress-induced depression. *Elife*. 2018;7:1-27. doi:10.7554/eLife.33273
50. Hu P, Maita I, Phan ML, et al. Early-life stress alters affective behaviors in adult mice through persistent activation of CRH-BDNF signaling in the oval bed nucleus of the stria terminalis. *Transl Psychiatry*. 2020b;10(1):396. doi:10.1038/s41398-020-01070-3
51. Hodes GE. A primer on sex differences in the behavioral response to stress. *Curr Opin Behav Sci*. 2018;23:75-83. doi:10.1016/j.cobeha.2018.03.012
52. Mineur YS, Belzung C, Crusio WE. Effects of unpredictable chronic mild stress on anxiety and depression-like behavior in mice. *Behav Brain Res*. 2006;175(1):43-50. doi:10.1016/j.bbr.2006.07.029
53. Greger IH, Watson JF, Cull-Candy SG. Structural and functional architecture of AMPA-type glutamate receptors and their auxiliary proteins. *Neuron*. 2017;94(4):713-730. doi:10.1016/j.neuron.2017.04.009
54. Coombs ID, Cull-Candy SG. Transmembrane AMPA receptor regulatory proteins and AMPA receptor function in the cerebellum. *Neuroscience*. 2009;162(3):656-665. doi:10.1016/j.neuroscience.2009.01.004
55. Johnson CP, Chapman ER. Otoferlin is a calcium sensor that directly regulates SNARE-mediated membrane fusion. *J Cell Biol*. 2010;191(1):187-197. doi:10.1083/jcb.201002089
56. Inagaki N, Chihara K, Arimura N, et al. CRMP-2 induces axons in cultured hippocampal neurons. *Nat Neurosci*. 2001;4(8):781-782. doi:10.1038/90476
57. Jang S, Oh D, Lee Y, et al. Synaptic adhesion molecule IgSF11 regulates synaptic transmission and plasticity. *Nat Neurosci*. 2016;19(1):84-93. doi:10.1038/nn.4176
58. Ma K, Zhang H, Wei G, et al. Identification of key genes, pathways and miRNA/mRNA regulatory networks of CUMS-induced depression in nucleus accumbens by integrated bioinformatics analysis. *Neuropsychiatr Dis Treat*. 2019;15:685-700. doi:10.2147/NDT.S200264
59. Karisetty BC, Khandelwal N, Kumar A, Chakravarty S. Sex difference in mouse hypothalamic transcriptome profile in stress-induced depression model. *Biochem Biophys Res Commun*. 2017;486(4):1122-1128. doi:10.1016/j.bbrc.2017.04.005
60. Yang S, Yi L, Xia X, et al. Transcriptome comparative analysis of amygdala-hippocampus in depression: a rat model induced by chronic unpredictable mild stress (CUMS). *J Affect Disord*. 2023;334:258-270. doi:10.1016/j.jad.2023.04.074
61. Hu Y, Liu Y, Quan X, Fan W, Xu B, Li S. RBM3 is an outstanding cold shock protein with multiple physiological functions beyond hypothermia. *J Cell Physiol*. 2022;237(10):3788-3802. doi:10.1002/jcp.30852
62. Egli RE, Winder DG. Dorsal and ventral distribution of excitable and synaptic properties of neurons of the bed nucleus of the stria terminalis. *J Neurophysiol*. 2003;90(1):405-414. doi:10.1152/jn.00228.2003
63. Wu X-S, Xue L, Mohan R, Paradiso K, Gillis KD, Wu L-G. The origin of quantal size variation: vesicular glutamate concentration plays a significant role. *J Neurosci*. 2007;27(11):3046-3056. doi:10.1523/jneurosci.4415-06.2007
64. Pulido C, Marty A. Quantal fluctuations in central mammalian synapses: functional role of vesicular docking sites. *Physiol Rev*. 2017;97(4):1403-1430. doi:10.1152/physrev.00032.2016
65. He L, Xue L, Xu J, et al. Compound vesicle fusion increases quantal size and potentiates synaptic transmission. *Nature*. 2009;459(7243):93-97. doi:10.1038/nature07860
66. Auger C, Marty A. Quantal currents at single-site central synapses. *J Physiol*. 2000;526(1):3-11. doi:10.1111/j.1469-7793.2000.t01-3-00003.x
67. Ventriglia F, Di Maio V. Stochastic fluctuations of the synaptic function. *Biosystems*. 2002;67(1):287-294. doi:10.1016/S0303-2647(02)00086-2
68. Ventriglia F, Di Maio V. Stochastic fluctuations of the quantal EPSC amplitude in computer simulated excitatory synapses of hippocampus. *Biosystems*. 2003;71(1):195-204. doi:10.1016/S0303-2647(03)00117-5
69. Han EB, Stevens CF. Development regulates a switch between post- and presynaptic strengthening in response to activity deprivation. *Proc Natl Acad Sci*. 2009;106(26):10817-10822. doi:10.1073/pnas.0903603106
70. Sun Y, Zweifel LS, Holmes TC, Xu X. Whole-brain input mapping of the lateral versus medial anterodorsal bed nucleus of the stria terminalis in the mouse. *Neurobiol Stress*. 2023;23:100527. doi:10.1016/j.ynstr.2023.100527

SUPPORTING INFORMATION

Additional supporting information can be found online in the Supporting Information section at the end of this article.

How to cite this article: Degroat TJ, Paladino SE, Samuels BA, Roepke TA. Chronic variable mild stress alters the transcriptome and signaling properties of the anterodorsal bed nucleus of the stria terminalis in a sex-dependent manner. *J Neuroendocrinol*. 2025;37(8):e70041. doi:10.1111/jne.70041

13652826, 2025, 8, Downloaded from https://onlinelibrary.wiley.com/doi/10.1111/jne.70041 by Benjamin Samuels - Rutgers University Libraries , Wiley Online Library on [07/11/2026]. See the Terms and Conditions (https://onlinelibrary.wiley.com/terms-and-conditions) on Wiley Online Library for rules of use; OA articles are governed by the applicable Creative Commons License